A combinatorial description
of knot Floer homology

By Ciprian Manolescu, Peter Ozsváth, and Sucharit Sarkar*

Abstract

Given a grid presentation of a knot (or link) K in the three-sphere, we describe a Heegaard diagram for the knot complement in which the Heegaard surface is a torus and all elementary domains are squares. Using this diagram, we obtain a purely combinatorial description of the knot Floer homology of K.

1. Introduction

Heegaard Floer homology [24] is an invariant for three-manifolds, defined using holomorphic disks and Heegaard diagrams. In [23] and [27], this construction is extended to give an invariant, *knot Floer homology* $\widehat{\mathrm{HFK}}$, for null-homologous knots in a closed, oriented three-manifold. This construction is further generalized in [25] to the case of oriented links. The definition of all these invariants involves counts of holomorphic disks in the symmetric product of a Riemann surface, which makes them rather challenging to calculate.

In its most basic form, knot Floer homology is an invariant for knots $K \subset S^3$, $\widehat{\mathrm{HFK}}(K)$, which is a finite-dimensional bi-graded vector space over $\mathbb{F} = \mathbb{Z}/2\mathbb{Z}$, i.e.

$$\widehat{\mathrm{HFK}}(K) = \bigoplus_{m,s} \widehat{\mathrm{HFK}}_m(K,s).$$

This invariant is related to the symmetrized Alexander polynomial $\Delta_K(T)$ by the formula

$$(1) \qquad \Delta_K(T) = \sum_{m,s} (-1)^m \mathrm{rank}\, \widehat{\mathrm{HFK}}_m(K,s) \cdot T^s$$

(cf. [23], [27]). The topological significance of this invariant is illustrated by the result that

$$g(K) = \max\{s \in \mathbb{Z} \,|\, \widehat{\mathrm{HFK}}_*(K,s) \neq 0\},$$

where here $g(K)$ denotes the Seifert genus of K (cf. [22]), and also the fact that $\widehat{\mathrm{HFK}}_*(K, g(K))$ has rank one if and only if K is fibered ([10] in the case where $g(K) = 1$ and [19] in general). The invariant is defined as a version of Lagrangian Floer homology [6] in a suitable symmetric product of a Heegaard surface.

Our aim here is to give a purely combinatorial presentation of knot Floer homology with coefficients in $\mathbb{F}$ for knots in the three-sphere. Our description can be extended to describe link Floer homology, and also it can be extended to describe the "full knot filtration" (and in particular the concordance invariant τ [21]). However, in the interest of exposition, we limit ourselves in the introduction to the case of knot Floer homology, referring the interested reader to Section 3 for more general cases.

To explain our combinatorial description, it will be useful to have the following notions.

A *planar grid diagram* $\widetilde{\Gamma}$ consists of a square grid on the the plane with $n \times n$ cells, together with a collection of black and white dots on it, arranged so that:

- every row contains exactly one black dot and one white dot;
- every column contains exactly one black dot and one white dot;
- no cell contains more than one dot.

The number n is called the *grid number* of $\widetilde{\Gamma}$.

Given a planar grid diagram $\widetilde{\Gamma}$, we can place it in a standard position on the plane as follows: the bottom left corner is at the origin, each cell is a square of edge length one, and every dot is in the middle of the respective cell. We then construct a planar knot projection by drawing horizontal segments from the white to the black dot in each row, and vertical segments from the black to the white dot in each column. At every intersection point, we let the horizontal segment be the underpass and the vertical one the overpass. This produces a planar diagram for an oriented link $\vec{L}$ in S^3. We say that $\vec{L}$ has a grid presentation given by $\widetilde{\Gamma}$. Figure 1 shows a grid presentation of the trefoil, with $n = 5$.

It is easy to see that every knot (or link) in the three-sphere can be presented by a planar grid diagram. In fact, grid presentations are equivalent to the arc presentations of knots, which first appeared in [1], the square bridge positions of knots of [15], and also to Legendrian realizations of knots, cf. [17]; they have enjoyed a considerable amount of attention over the years (see also [3], [4]). The minimum number n for which a knot $K \subset S^3$ admits a grid presentation of grid number n is called the *arc index* of K.

We find it convenient to transfer our planar grid diagrams to the torus $\mathcal{T}$ obtained by gluing the top-most segment to the bottom-most one, and the left-most segment to the right-most one. In the torus, our horizontal and vertical
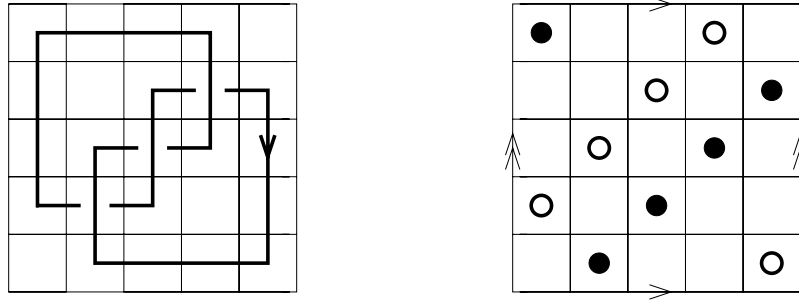
Figure 1: *Grid diagram for the trefoil.* We have pictured here a grid diagram for the trefoil, with projection indicated on the left. To pass from a planar to a toroidal grid diagram, we make the identifications suggested by the arrows.

arcs become horizontal and vertical circles. The torus inherits its orientation from the plane. We call the resulting object Γ a *toroidal grid diagram*, or simply a grid diagram, for K.

Given a toroidal grid diagram, we associate to it a chain complex $\big(C(\Gamma), \partial\big)$ as follows. The generators X of $C(\Gamma)$ are indexed by one-to-one correspondences between the horizontal and vertical circles. More geometrically, we can think of these as n-tuples of intersection points $\mathbf{x}$ between the horizontal and vertical circles, with the property that no intersection point appears on more than one horizontal (or vertical) circle.

We now define functions $A\colon X \longrightarrow \mathbb{Z}$ and $M\colon X \longrightarrow \mathbb{Z}$ (the Alexander and Maslov gradings) as follows.

Let us define a function a on lattice points p to be minus one times the winding number of the knot projection around p. (This is shown in Figure 2 for our trefoil example.) Each black or white dot in the diagram lies in a square. We thus obtain $2n$ distinguished squares, and each of them has four corners. We denote the resulting collection of corners $\{c_{i,j}\}$, $i \in \{1, \ldots, 2n\}$, $j \in \{1, \ldots, 4\}$. We set

$$(2) \qquad A(\mathbf{x}) = \sum_{p \in \mathbf{x}} a(p) - \frac{1}{8}\Big(\sum_{i,j} a(c_{i,j})\Big) - \frac{n-1}{2}.$$

Next, given a pair of generators $\mathbf{x}$ and $\mathbf{y}$, and an embedded rectangle r in $\mathcal{T}$ whose edges are arcs in the horizontal and vertical circles, we say that r connects $\mathbf{x}$ to $\mathbf{y}$ if $\mathbf{x}$ and $\mathbf{y}$ agree along all but two horizontal circles, if all four corners of r are intersection points in $\mathbf{x} \cup \mathbf{y}$. If we traverse each horizontal boundary components of r in the direction dictated by the orientation that r inherits from $\mathcal{T}$, then the arc is oriented so as to go from a point in $\mathbf{x}$ to the point in $\mathbf{y}$. Let $R_{\mathbf{x},\mathbf{y}}$ denote the collection of rectangles connecting $\mathbf{x}$ to $\mathbf{y}$.
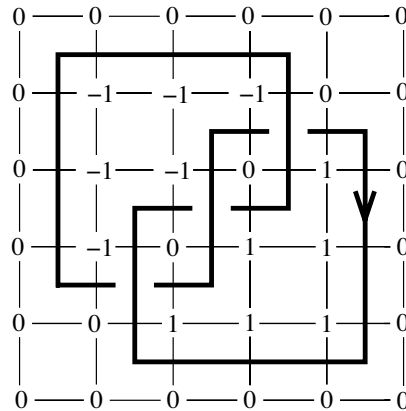
Figure 2: *The function a.* Over every lattice point p from Figure 1, we marked minus the winding number of the knot projection around p.
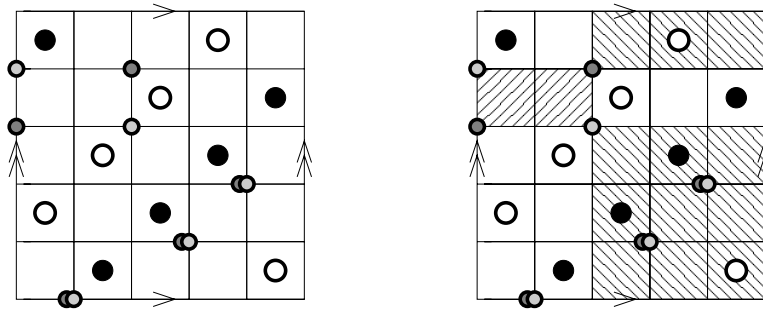

Figure 3: *Rectangles.* At the left, we have indicated two generators $\mathbf{x}$ and $\mathbf{y}$ in X for the grid diagram of the trefoil considered earlier. The generators $\mathbf{x}$ and $\mathbf{y}$ are represented by the collections of (smaller) shaded dots centered on the intersection points of the grid, with $\mathbf{x}$ represented by the more darkly shaded circles and $\mathbf{y}$ represented by the more lightly shaded ones. Note that three dots in $\mathbf{x}$ occupy the same locations on the grid as $\mathbf{y}$-dots, while two do not. At the right, we have have indicated the two rectangles in $R_{\mathbf{x},\mathbf{y}}$, which are shaded by (the two types of) diagonal hatchings. One of these rectangles r has $P_{\mathbf{x}}(r) + P_{\mathbf{y}}(r) = 1$ and $W(r) = B(r) = 0$ (and hence it represents a nontrivial differential from $\mathbf{x}$ to $\mathbf{y}$), while the other rectangle r' has $P_{\mathbf{x}}(r') + P_{\mathbf{y}}(r') = 5$ and $W(r') = B(r') = 2$.

It is easy to see that if $\mathbf{x}, \mathbf{y} \in X$, and if $\mathbf{x}$ and $\mathbf{y}$ differ along exactly two horizontal circles, then there are exactly two rectangles in $R_{\mathbf{x},\mathbf{y}}$; otherwise $R_{\mathbf{x},\mathbf{y}} = \emptyset$ (cf. Figure 3).

Given $\mathbf{x}, \mathbf{y} \in X$, it is easy to find an oriented, null-homologous curve $\gamma_{\mathbf{x},\mathbf{y}}$ composed of horizontal and vertical arcs, where each horizontal arc goes from a point in $\mathbf{x}$ to a point in $\mathbf{y}$ (and hence each vertical arc goes from a point in $\mathbf{y}$ to a point in $\mathbf{x}$). Now, suppose that D is a two-chain whose boundary is a collection of horizontal and vertical arcs, and $\mathbf{x} \in X$. We let $W(D)$ and $B(D)$ denote the number of white and black dots in D respectively. Moreover, near each intersection point x of the horizontal and vertical circles, D has four local multiplicities. We define the local multiplicity of D at x, $p_x(D)$, to be the average of these four local multiplicities. Moreover, given $\mathbf{x} \in X$, let

$$P_{\mathbf{x}}(D) = \sum_{x \in \mathbf{x}} p_x(D).$$

Now, M is uniquely characterized up to an additive constant by the property that for each $\mathbf{x}, \mathbf{y} \in X$,

$$(3) \qquad M(\mathbf{x}) - M(\mathbf{y}) = P_{\mathbf{x}}(D) + P_{\mathbf{y}}(D) - 2 \cdot W(D),$$

where here D is some two-chain whose boundary is $\gamma_{\mathbf{x},\mathbf{y}}$. (Observe that we have displayed here a simple special case of Lipshitz's formula for the Maslov index of a holomorphic disk in the symmetric product, cf. [14].) Note that the right-hand side is independent of the choice of D, as follows. Let $\{A_i\}_{i=1}^n$ and $\{B_i\}_{i=1}^n$ be the annuli given by $\Sigma - \alpha_1 - \cdots - \alpha_n$ and $\beta_1 - \cdots - \beta_n$ respectively. Note that any two choices of D and D' connecting $\mathbf{x}$ to $\mathbf{y}$ differ by adding or subtracting a finite number of annuli A_i and B_j. But for each such annulus A, $P_{\mathbf{x}}(A) = 1$, $P_{\mathbf{y}}(A) = 1$, and $W(A) = 1$, and hence they do not change the right-hand side. Moreover, the additive indeterminacy in M is removed by the following convention. Consider the generator $\mathbf{x}_0$ which occupies the lower left-hand corner of each square which contains a white dot; cf. Figure 4. We declare that $M(\mathbf{x}_0) = 1 - n$.

Consider $C(\Gamma)$, the $\mathbb{F}$-vector space generated by elements of X. We define a differential

$$\partial \colon C(\Gamma) \longrightarrow C(\Gamma)$$

by the formula

$$\partial \mathbf{x} = \sum_{\mathbf{y} \in X} \sum_{r \in R_{\mathbf{x},\mathbf{y}}} \left\{ \begin{array}{ll} 1 & \text{if } P_{\mathbf{x}}(r) + P_{\mathbf{y}}(r) = 1 \text{ and } W(r) = B(r) = 0 \\ 0 & \text{otherwise} \end{array} \right\} \cdot \mathbf{y}.$$

The condition that $P_{\mathbf{x}}(r) + P_{\mathbf{y}}(r) = 1$ and $W(r) = B(r) = 0$ is, of course, equivalent to the condition that the interior of the rectangle r contains no black points, white points, or points amongst the $\mathbf{x}$ and $\mathbf{y}$.
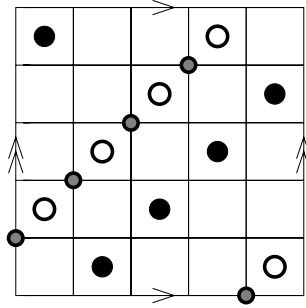
Figure 4: *The generator* $\mathbf{x}_0$. We have illustrated here the generator with Maslov grading equal to $1 - n$.

It is easy to see that ∂ drops Maslov grading by one and preserves Alexander grading. It is also elementary to verify that $\partial^2 = 0$. Thus, we can take the homology of this complex to obtain a bigraded vector space over $\mathbb{F}$.

Let V be the two-dimensional bigraded vector space spanned by one generator in bigrading $(-1, -1)$ and another in bigrading $(0, 0)$.

We can now state the following:

THEOREM 1.1. *Fix a grid presentation* Γ *of a knot* K, *with grid number* n. *Then, the homology of the above chain complex* $H_*(C(\Gamma), \partial)$ *is isomorphic to the bigraded group* $\widehat{\mathrm{HFK}}(K) \otimes V^{\otimes(n-1)}$.

The key point of the above theorem is to find a suitable Heegaard diagram for S^3 compatible with the knot K. Indeed, the diagram we use has genus one, with Heegaard torus $\mathcal{T}$, and K is represented as a collection of horizontal and vertical arcs. This Heegaard diagram has the property that the knot pierces $\mathcal{T}$ in several pairs of points, and the very interesting property that the complement in $\mathcal{T}$ of the attaching circles is a collection of squares. In this case, properties of the Maslov index ensure that the only holomorphic disks are rectangles. Thus the chain complex $C(\Gamma)$ we have described above agrees with the Heegaard Floer complex for this diagram.

There are several other variants of Theorem 1.1. There is, for example, a version which calculates $\widehat{\mathrm{HFK}}(K)$ directly (though it is uniquely determined by the above result), except there one needs to consider a variant of the above the chain complex defined over a suitable polynomial algebra.

In this paper, we also consider several other versions of Theorem 1.1. We discuss how to calculate the other variants of knot Floer homology, and also a variant for links.

This paper is organized as follows. In Section 2, we describe the construction of link Floer homology using Heegaard diagrams with the property that the link crosses the Heegaard surface in many points. This construction is then identified with the usual construction using methods from [25]. In Section 3,

we identify the chain complex $C(\Gamma)$ with the link Floer homology complex using the toroidal grid diagram of L, interpreted as a Heegaard diagram for L, and state some more general consequences. Finally, in Section 4, we describe some simple examples to illustrate our results.

Further remarks. Whereas the constructions in this paper give a purely combinatorial chain complex for knot Floer homology, Theorem 1.1 is still somewhat impractical, as the chain complex $C(\Gamma)$ typically has far too many generators: for a knot with arc index n, the procedure gives a chain complex with $n!$ generators. It remains a very interesting challenge to come up with more efficient methods for calculating the homology of the complexes we describe here.

In a different direction, the relationship between our combinatorial description and Legendrian knots seems tantalizing: one wonders whether this is perhaps the hint of a connection with the holomorphic invariants of those objects; compare [2], [5], [18].

We would like to remind the reader that we have kept the introduction as elementary as possible. The more general results of Section 3 actually lead to a calculation of link Floer homology for links in S^3. Also, the extra data about the "knot filtration" allows one to calculate the concordance invariant τ for knots. It is also the input needed to determine the ranks of Heegaard Floer homology groups of Dehn surgeries on a given knot K; see [26].

2. Link Floer homology with multiple basepoints

We review here the construction of knot and link Floer homology, considering the case where the link meets the Heegaard surface in extra intersection points. The fact that Heegaard Floer homology can be extracted from this picture follows essentially from [25].

Let $(\Sigma, \boldsymbol{\alpha}, \boldsymbol{\beta}, \mathbf{w}, \mathbf{z})$ be a Heegaard diagram, where Σ is a surface of genus g, k is some positive integer, $\boldsymbol{\alpha} = \{\alpha_1, \ldots, \alpha_{g+k-1}\}$ are pairwise disjoint, embedded curves in Σ which span a half-dimensional subspace of $H_1(\Sigma; \mathbb{Z})$ (and hence specify a handlebody U_α with boundary equal to Σ), $\boldsymbol{\beta} = \{\beta_1, \ldots, \beta_{g+k-1}\}$ is another collection of attaching circles specifying U_β, and $\mathbf{w} = \{w_1, \ldots, w_k\}$ and $\mathbf{z} = \{z_1, \ldots, z_k\}$ are distinct marked points with

$$\mathbf{w}, \mathbf{z} \subset \Sigma - \alpha_1 - \cdots - \alpha_{g+k-1} - \beta_1 - \cdots - \beta_{g+k-1}.$$

The data $(\Sigma, \boldsymbol{\alpha}, \boldsymbol{\beta})$ specifies a Heegaard splitting for some oriented three-manifold Y. In the present applications, we will be interested in the case where the ambient three-manifold is the three-sphere, and hence, we make this assumption hereafter.

Let $\{A_i\}_{i=1}^k$ resp. $\{B_i\}_{i=1}^k$ be the connected components of $\Sigma - \alpha_1 - \cdots - \alpha_{g+k-1}$ resp. $\Sigma - \beta_1 - \cdots - \beta_{g+k-1}$.

We suppose that our basepoints are placed in such a manner that each component A_i or B_i contains exactly one basepoint amongst the $\mathbf{w}$ and exactly one basepoint amongst the $\mathbf{z}$. We can label our basepoints so that A_i contains z_i and w_i, and then B_i contains w_i and $z_{\nu(i)}$, for some permutation ν of $\{1, \ldots, k\}$.

In this case, the basepoints uniquely specify an oriented link L in $S^3 = U_\alpha \cup U_\beta$, by the following conventions. For each $i = 1, \ldots, k$, let ξ_i denote an arc in A_i from z_i to w_i and let η_i denote an arc in B_i from w_i to $z_{\nu(i)}$. Let $\widetilde{\xi}_i \subset U_\alpha$ be an arc obtained by pushing the interior of ξ_i into U_α, and $\widetilde{\eta}_i$ be the arc obtained by pushing the interior of η_i into U_β. Now, we can let L be the oriented link obtained as the sum

$$\bigcup_{i=1}^k \left(\widetilde{\xi}_i + \widetilde{\eta}_i \right).$$

Definition 2.1. In the above case, we say that $(\Sigma, \boldsymbol{\alpha}, \boldsymbol{\beta}, \mathbf{w}, \mathbf{z})$ is a $2k$-pointed Heegaard diagram compatible with the oriented link L in S^3.

Let ℓ denote the number of components of L. Clearly, $k \geq \ell$. In the case where $k = \ell$, these are the Heegaard diagrams used in the definition of link Floer homology [25]; see also [23], [27]. In the case where $k > \ell$, these Heegaard diagrams can still be used to calculate link Floer homology, in a suitable sense.

Definition 2.2. A *periodic domain* is a two-chain of the form

$$P = \sum_{i=1}^k (a_i \cdot A_i + b_i \cdot B_i)$$

which has zero local multiplicity at all of the $\{w_i\}_{i=1}^k$. A Heegaard diagram is said to be *admissible* if every nontrivial periodic domain has some positive local multiplicities and some negative local multiplicities.

Consider first the case where our link is in fact a knot. In this case, admissibility is automatically satisfied. Specifically, if we introduce cyclic orderings of $\{A_i\}_{i=1}^k$ and $\{B_i\}_{i=1}^k$, $\{w_i\}_{i=1}^k$ and $\{z_i\}_{i=1}^k$, so that $w_i, z_i \in A_i$ and $w_i, z_{i+1} \in B_i$, then $n_{w_i}(P) = a_i + b_i$ and $n_{z_i}(P) = a_i + b_{i-1}$. The condition that P is a periodic domain ensures that for each i, $a_i + b_i = 0$. Thus, if for some i we have $n_{z_i}(P) > 0$ (i.e. $a_i + b_{i-1} > 0$) then for some other j, $n_{z_j}(P) = a_j + b_{j-1} < 0$. Conversely, if $n_{w_i}(P) = n_{z_i}(P) = 0$ for all i, then there is some constant c with all $a_i = c = -b_i$; it follows readily that $P = 0$.

Let $(\Sigma, \boldsymbol{\alpha}, \boldsymbol{\beta}, \mathbf{w}, \mathbf{z})$ be a Heegaard diagram compatible with an oriented knot K. We will consider Floer homology in the $g + k - 1$-fold symmetric product of the surface Σ, relative to the pair of totally real submanifolds

$$\mathbb{T}_\alpha = \alpha_1 \times \cdots \times \alpha_{g+k-1} \text{ and } \mathbb{T}_\beta = \beta_1 \times \cdots \times \beta_{g+k-1}.$$

Given $\mathbf{x}, \mathbf{y} \in \mathbb{T}_\alpha \cap \mathbb{T}_\beta$, let $\pi_2(\mathbf{x}, \mathbf{y})$ denote the space of homology classes of Whitney disks from $\mathbf{x}$ to $\mathbf{y}$, i.e. maps of the standard complex disk into $\mathrm{Sym}^{g+k-1}(\Sigma)$ which carry i resp. $-i$ to $\mathbf{x}$ resp. $\mathbf{y}$, and points on the circle with negative resp. positive real part to $\mathbb{T}_\alpha$ resp. $\mathbb{T}_\beta$. (Note that when $g + k > 3$, homology classes of Whitney disks agree with homotopy classes.)

We consider now the chain complex $\mathrm{CFK}^-(\Sigma, \boldsymbol{\alpha}, \boldsymbol{\beta}, \mathbf{w}, \mathbf{z})$ over the polynomial algebra $\mathbb{F}[U_1, \ldots, U_k]$ which is freely generated by intersection points between the tori $\mathbb{T}_\alpha = \alpha_1 \times \cdots \times \alpha_{g+k-1}$ and $\mathbb{T}_\beta = \beta_1 \times \cdots \times \beta_{g+k-1}$ in $\mathrm{Sym}^{g+k-1}(\Sigma)$. This module is endowed with the differential

$$(4) \quad \partial^- \mathbf{x} = \sum_{\mathbf{y} \in \mathbb{T}_\alpha \cap \mathbb{T}_\beta} \sum_{\{\phi \in \pi_2(\mathbf{x}, \mathbf{y}) \mid \mu(\phi) = 1\}} \# \left(\frac{\mathcal{M}(\phi)}{\mathbb{R}} \right) U_1^{n_{w_1}(\phi)} \cdot \ldots \cdot U_k^{n_{w_k}(\phi)} \cdot \mathbf{y},$$

where, as usual, $\pi_2(\mathbf{x}, \mathbf{y})$ denotes the space of homology classes of Whitney disks connecting $\mathbf{x}$ to $\mathbf{y}$, $\mathcal{M}(\phi)$ denotes the moduli space of pseudo-holomorphic representatives of ϕ, $\mu(\phi)$ denotes its formal dimension (Maslov index), $n_p(\phi)$ denotes the local multiplicity of ϕ at the reference point p (i.e. the algebraic intersection number of ϕ with the subvariety $\{p\} \times \mathrm{Sym}^{g+k-2}(\Sigma)$), and $\#()$ denotes a count modulo two. As usual, in the definition of pseudo-holomorphic disks, one uses a suitable perturbation of the condition on the disk that it be holomorphic with respect to the complex structure on $\mathrm{Sym}^{g+k-1}(\Sigma)$ induced from some complex structure on Σ, as explained in [24, §3]; see also [7], [20], [8], [9] for more general discussions. We use here a sufficiently small perturbation to retain the property that if u is pseudo-holomorphic, then for all $p \in \Sigma - \alpha_1 - \cdots - \alpha_{g+k-1} - \beta_1 - \cdots - \beta_{g+k-1}$, $n_p(\phi) \geq 0$; cf. [24, Lemma 3.2]. For the case where the Heegaard diagram is admissible, it is easy to see that Equation (4) gives a finite sum; compare [24].

The *relative Alexander grading* of two intersection points $\mathbf{x}$ and $\mathbf{y}$ is defined by the formula

$$(5) \qquad A(\mathbf{x}) - A(\mathbf{y}) = \left(\sum_{i=1}^n n_{z_i}(\phi) \right) - \left(\sum_{i=1}^n n_{w_i}(\phi) \right),$$

where $\phi \in \pi_2(\mathbf{x}, \mathbf{y})$ is any homotopy class from $\mathbf{x}$ to $\mathbf{y}$. We find it convenient to remove the additive indeterminacy in A: there is a unique choice with the property that

$$(6) \qquad \sum_{\mathbf{x} \in \mathbb{T}_\alpha \cap \mathbb{T}_\beta} T^{A(\mathbf{x})} \equiv \Delta_K(T) \cdot (1 - T^{-1})^{n-1} \pmod 2,$$

where $\Delta_K(T)$ is the symmetrized Alexander polynomial which could be made to work over $\mathbb{Z}$ by introducing signs. (These conventions are chosen to be consistent with those made in Proposition 2.3 below.)

Moreover, there is a *relative Maslov grading*, defined by

$$(7) \qquad M(\mathbf{x}) - M(\mathbf{y}) = \mu(\phi) - 2 \sum_{i=1}^n n_{w_i}(\phi).$$

The relative Maslov grading can be lifted to an absolute grading using the observation that $(\Sigma, \boldsymbol{\alpha}, \boldsymbol{\beta}, \mathbf{w})$ is a multiply-pointed Heegaard diagram for S^3 (a *balanced n-pointed Heegaard diagram* in the terminology of [25]), and consequently, if one sets all the $U_i = 0$, the homology groups of the resulting complex, one obtains a relatively graded group which is isomorphic to $H_*(T^{k-1}; \mathbb{F})$ (compare [25, Th. 4.5]). The Maslov grading is fixed by the requirement that

$$(8) \qquad H_*(\mathrm{CFK}^-/\{U_i = 0\}) \cong H_{*+k-1}(T^{k-1}; \mathbb{F}).$$

So far, we have made no reference to the basepoints $\mathbf{z}$. Indeed, the complex $\mathrm{CF}^-(\Sigma, \boldsymbol{\alpha}, \boldsymbol{\beta}, \mathbf{w}, \mathbf{z})$ so far is the chain complex for $\mathrm{HF}^-(S^3)$ for a multi-pointed Heegaard diagram, in the sense of [25, §4.5].

This complex admits an *Alexander filtration* defined by the convention that any element $\mathbf{x} \in \mathbb{T}_\alpha \cap \mathbb{T}_\beta$ has Alexander filtration level $A(\mathbf{x})$, and multiplication by the variables U_i drops Alexander filtration by one, i.e.

$$A(U_1^{a_1} \cdot \ldots \cdot U_k^{a_k} \cdot \mathbf{x}) = A(\mathbf{x}) - a_1 - \cdots - a_k.$$

Nonnegativity of local multiplicities of pseudo-holomorphic disks ensures that this function indeed defines a filtration on the complex; i.e., we have an increasing sequence of subcomplexes $\mathcal{F}^-(K, m) \subset \mathrm{CFK}^-(K)$ indexed by integers m, which are generated over $\mathbb{F}[U_1, \ldots, U_k]$ by intersection points $\mathbf{x}$ with $A(\mathbf{x}) \leq m$.

In the case where $k = 1$, the above construction gives the chain homotopy type of the "knot filtration" on $\mathrm{CF}^-(S^3)$, called $\mathrm{CFK}^-(K)$, which is a chain complex over the polynomial algebra $\mathbb{F}[U]$. In this case, it was shown in [23]

and [27] that the filtered chain homotopy type of the complex is a knot invariant. Our goal here is to show that this filtered chain homotopy type is also independent of k.

In practice, it is often more convenient to consider the simpler complex $C(\Sigma, \boldsymbol{\alpha}, \boldsymbol{\beta}, \mathbf{w}, \mathbf{z})$ generated by intersection points of $\mathbb{T}_\alpha$ and $\mathbb{T}_\beta$ with coefficients in $\mathbb{F}$, endowed with the differential

$$\partial \mathbf{x} = \sum_{\mathbf{y} \in \mathbb{T}_\alpha \cap \mathbb{T}_\beta} \sum_{\{\phi \in \pi_2(\mathbf{x}, \mathbf{y}) \big| \begin{subarray}{c} \mu(\phi) = 1, \\ n_{w_i}(\phi) = n_{z_i}(\phi) = 0 \end{subarray} \quad \forall i = 1, \ldots, n \}} \# \left(\frac{\mathcal{M}(\phi)}{\mathbb{R}} \right) \cdot \mathbf{y}.$$

For this complex, the function A defines an Alexander grading which is preserved by the differential. One can think of $C(\Sigma, \boldsymbol{\alpha}, \boldsymbol{\beta}, \mathbf{w}, \mathbf{z})$ as obtained from $\mathrm{CFK}^-(\Sigma, \boldsymbol{\alpha}, \boldsymbol{\beta}, \mathbf{w}, \mathbf{z})$ by first setting all the $U_i = 0$, and then taking the graded object associated to the Alexander filtration.

The following proposition shows how to extract the usual knot Floer homology from the above variants using multiple basepoints. The result is an adaptation of the results from [25, §6.1], but we sketch the proof here for the reader's convenience.

PROPOSITION 2.3. *Let* $(\Sigma, \boldsymbol{\alpha}, \boldsymbol{\beta}, \mathbf{w}, \mathbf{z})$ *be a* $2k$-*pointed Heegaard diagram compatible with a knot* K. *Then, the filtered chain homotopy type of* $\mathrm{CFK}^-(\Sigma, \boldsymbol{\alpha}, \boldsymbol{\beta}, \mathbf{w}, \mathbf{z})$, *thought of as a complex over* $\mathbb{F}[U]$ *where* U *can be any* U_i, *agrees with the filtered chain homotopy type of* $\mathrm{CFK}^-(K)$. *Moreover, we have an identification*

$$(9) \qquad H_*(C(\Sigma, \boldsymbol{\alpha}, \boldsymbol{\beta}, \mathbf{w}, \mathbf{z}), \partial) \cong \widehat{HFK}(K) \otimes V^{\otimes(k-1)},$$

where V *is the two-dimensional vector space spanned by two generators, one in bigrading* $(-1, -1)$, *another in bigrading* $(0, 0)$.

We first establish the following:

LEMMA 2.4. *Let* k *be an integer greater than one. After a series of isotopies, handleslides and stabilizations, any* $2k$-*pointed Heegaard diagram* $(\Sigma, \boldsymbol{\alpha}, \boldsymbol{\beta}, \mathbf{w}, \mathbf{z})$ *compatible with a knot* K, *can be transformed into one with the following properties*:

- *there are curves* $\alpha_1 \in \boldsymbol{\alpha}$ *and* $\beta_1 \in \boldsymbol{\beta}$ *which bound disks* A_1 *and* B_1 *in* Σ;
- $A_1 \cap B_1$ *contains the basepoint* w_1;
- α_1 *and* β_1 *meet transversally in a pair of points*;
- α_1 *is disjoint from all* β_j *with* $j \neq 1$, *and* β_1 *is disjoint from all* α_j *with* $j \neq 1$.

Proof. Start from a $2k$ pointed Heegaard diagram $(\Sigma, \boldsymbol{\alpha}, \boldsymbol{\beta}, \mathbf{w}, \mathbf{z})$ compatible with K. Let A_1 be the component of $\Sigma - \boldsymbol{\alpha}_1 - \cdots - \boldsymbol{\alpha}_{g+k-1}$ which contains
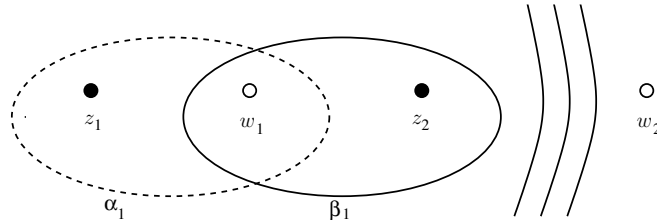
Figure 5: *Local picture near* w_1. We denote α_i by dashed and β_j by solid lines. The basepoint w_2 can be connected to z_2 by an arc which crosses β_1, and possibly a collection of other β-circles (but no α-circles).

$w_1 \in \mathbf{w}$, and B_1 be the component of $\Sigma - \boldsymbol{\beta}_1 - \cdots - \boldsymbol{\beta}_{g+k-1}$ containing w_1. In particular, if $z_1, z_2 \in \mathbf{z}$ are contained inside A_1 and B_1 respectively, then $z_1 \neq z_2$ (since otherwise the basepoints w_1 and z_1 would determine a closed, unknotted component of K and since K is a knot, we could conclude that K is the unknot and $k = 1$). After a sequence of handleslides amongst the $\boldsymbol{\alpha}$ and $\boldsymbol{\beta}$ which do not cross any of the basepoints $\mathbf{w}$, $\mathbf{z}$, we can reduce to the case where A_1 and B_1 are both disks. Let α_1 and β_1 denote the boundaries of A_1 and B_1 respectively.

Note that, since $z_1 = A_1 \cap \mathbf{z}$ and $z_2 = B_2 \cap \mathbf{z}$ and $z_1 \neq z_2$, the intersection $A_1 \cap B_1$ does not contain any $z_i \in \mathbf{z}$. In fact, the various arcs $A_1 \cap \beta_1$ divide A_1 into a collection of planar regions, one of which contains w_1, another of which contains z_1. All the other regions have no basepoints in them, and we call these *unmarked regions*. We can perform finger moves to eliminate all of the unmarked bigons in A_1, by which we mean unmarked regions in $A_1 - A_1 \cap \beta_1$ whose closure meets β_1 in a single component in A_1. Note that this might involve also cancelling intersection points betweeen α_1 with β_j for some $j \neq 1$ (see Figure 6). After doing this, $A_1 - A_1 \cap \beta_1$ consists of one region which is a bigon marked with w_1, another which is a bigon marked with z_1, and some unmarked regions which are all rectangles (i.e. their boundary meets β_1 in two components).

Now, $A_1 \cap B_1$ consists of a bigon marked with w_1 and a (possibly empty) collection of unmarked rectangles. We can reduce the number of unmarked rectangular regions in $A_1 \cap B_1$ by a stabilization, followed by four handleslides, as illustrated in Figure 7.

Finally, by performing handleslides of the additional α_i and β_j over α_1 and β_1 respectively (followed by some isotopies), we can arrange for the circles α_1 and β_1 to be disjoint from all the other α_i and β_j. $\qquad\square$

Proof of Proposition 2.3. We use induction on k. In the case where $k = 1$, there is nothing to prove.
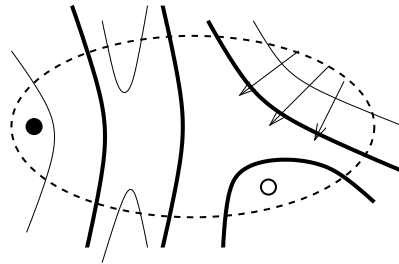
Figure 6: *Finger moves.* The circle α_1 is indicated by the dashed line. It bounds the disk A_1, which contains the basepoint w_1 (indicated by the hollow dot) and the basepoint z_1 (indicated by the dark dot). Other arcs belong to various β-circles, which divide A_1 into planar regions, with β_1 arcs denoted by the thicker lines and other β_j (with $j \neq 1$) by thinner ones. Performing the finger move on α_1 as indicated by the arrows, we can reduce the number of unmarked bigon regions in $A_1 - A_1 \cap \beta_1$.
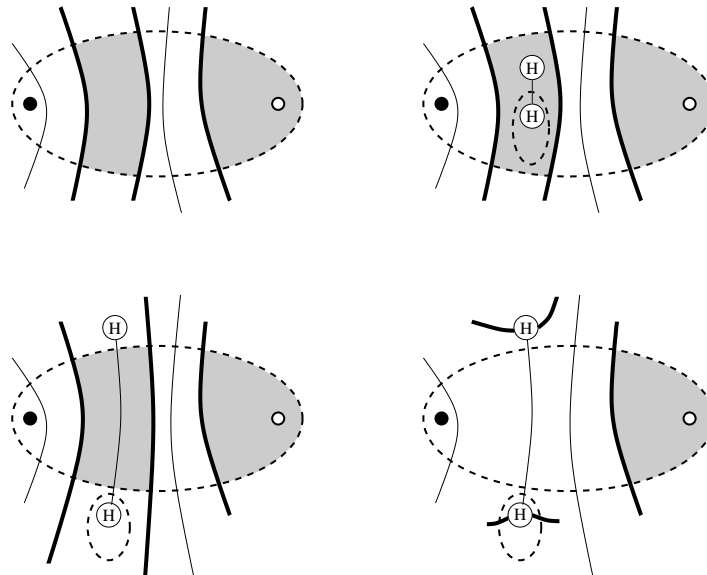

Figure 7: *Reducing rectangles in $A_1 \cap B_1$.* The dashed circle represents α_1, thick lines represent arcs from β_1, the thin arcs represent arcs from the other β_j (with $j \neq 1$), and the shaded regions represent $A_1 \cap B_1$. We eliminate the rectangular region in $A_1 \cap B_1$ by first stabilizing as in the second picture, introducing a new handle, represented by the two circles marked with H, along with the new dashed α-circle α_2, and the new β-circle β_2 indicated in the second picture by the thin arc running through the handle. Handlesliding α_1 over α_2 twice, we obtain the third picture. Handlesliding β_1 over β_2 twice, we end up with the fourth picture, which has one fewer (rectangular) component in $A_1 \cap B_1$.

When $k > 1$, using Lemma 2.4 we can reduce to the case where our diagram

$$(\Sigma, \boldsymbol{\alpha}, \boldsymbol{\beta}, \mathbf{w}, \mathbf{z})$$
$$= (\Sigma, \{\alpha_1, \ldots, \alpha_{g+k-1}\}, \{\beta_1, \ldots \beta_{g+k-1}\}, \{w_1, \ldots, w_k\}, \{z_1, \ldots, z_k\}),$$

has the special form in Figure 5. Note that under all the Heegaard moves used in Lemmaa 2.4, the filtered chain homotopy type of the associated chain complex remains invariant, as in [24], [23], [27].

We can de-stabilize the original diagram to get a $k - 1$-pointed Heegaard diagram

$$(\Sigma, \{\alpha_2, \ldots, \alpha_{g+k-1}\}, \{\beta_2, \ldots, \beta_{g+k-1}\}, \{w_2, \ldots, w_k\}, \{z_2, \ldots, z_k\})$$

for the same knot. Let C' denote its corresponding filtered Heegaard Floer complex

$$\mathrm{CFK}^-(\Sigma, \{\alpha_2, \ldots, \alpha_{g+k-1}\}, \{\beta_1, \ldots, \beta_{g+k-1}\}, \{w_2, \ldots, w_k\}, \{z_2, \ldots, z_k\}),$$

thought of as a module over the polynomial algebra $\mathbb{F}[U_2, \ldots, U_k]$. It is generated by the corresponding intersection points X' of the tori $\mathbb{T}'_\alpha$ and $\mathbb{T}'_\beta$ in $\mathrm{Sym}^{g+k-2}(\Sigma)$.

The set of generators X of the complex $\mathrm{CFK}^-(\Sigma, \boldsymbol{\alpha}, \boldsymbol{\beta}, \mathbf{w}, \mathbf{z})$ has the form $X' \times \{x, y\}$, where x and y are the two points of intersection of α_1 and β_1. Let C_x be the subgroup of C generated by intersection points of type $X' \times \{x\}$ and C_y be the subgroup generated by those of type $X' \times \{y\}$.

It is shown in the proof of [25, Prop. 6.5] that for a suitable choice of complex structure on Σ, the chain complex $\mathrm{CFK}^-(\Sigma, \boldsymbol{\alpha}, \mathbf{w}, \mathbf{z})$ is identified with the mapping cone of the chain map

$$(10) \qquad\qquad U_1 - U_2 \colon C'[U_1] \longrightarrow C'[U_1].$$

Here the domain is identified with C_x and the range with C_y. Specifically, under the natural identifications of groups $C_x \cong C'[U_1]$, $C_y \cong C'[U_1]$, we have that the differential of C is identified with the matrix

$$\begin{pmatrix} \partial' & U_1 - U_2 \\ 0 & \partial' \end{pmatrix},$$

where here the variable U_2 corresponds to the basepoint w_2 which lies in the same $\Sigma - \alpha_1 - \cdots - \alpha_{g+k-1}$-component as z_2. In this mapping cone, the Alexander filtration of a generator in $C'[U_1]$ thought of as supported in C_x is one higher than the Alexander filtration of the corresponding element, thought of as supported in C_y.

Let us say a few more words about the identification of $\mathrm{CFK}^-(\Sigma, \boldsymbol{\alpha}, \boldsymbol{\beta}, \mathbf{w}, \mathbf{z})$ with the mapping cone used above, referring the interested reader to [25, Prop. 6.5] for more details. Think of Σ as formed by the connected sum

of Σ' with a genus zero surface S containing both α_1 and β_1. Fixing con-
formal structures on Σ' and the sphere, we obtain a one-parameter family
of conformal structures on Σ by inserting a connected sum tube isometric to
$[0, T] \times S^1$, and allowing T to vary. When T is sufficiently large, the chain
complex $\mathrm{CFK}^-(\Sigma, \boldsymbol{\alpha}, \mathbf{w}, \mathbf{z})$ can be identified with the mapping cone of

$$U_1 - f \colon C'[U_1] \longrightarrow C'[U_1],$$

where f is a map which counts points in a fibered product of moduli spaces
of disks coming from Σ and S, fibered over a nontrivial symmetric product
of the disk, where the maps are obtained as the preimage of the connected
sum points p and q in Σ' and S. (The term U_1 fits into this picture formally
as the fibered product over the empty symmetric product.) To understand f
(and identify it with U_2), we must consider a second parameter s in the space
of conformal structures on Σ, which is given by moving the connected sum
point q in S. Indeed, it will be useful to move the connected sum point $q \in S$
towards α_1 (so that as $s \mapsto \infty$, q limits onto α_1). In fact, for q sufficiently
close to α_1 (i.e. s sufficiently large), the only nonempty moduli space which
contributes to this fiber product consists of holomorphic disks in $\mathrm{Sym}^{g+k-2}(\Sigma)$
with Maslov index equal to two which carry some fixed point m in the disk
(whose distance to the α-boundary of the disk goes to zero as $s \mapsto \infty$) into
$q \times \mathrm{Sym}^{g+k-3}$. When m is sufficiently close to the α-boundary, the count
of these disks is identified with the count of Maslov index two α-boundary
degenerations for Σ with local multiplicity 1 at the connected sum point p.
The contribution of these boundary degenerations is given by multiplication
by U_2. This gives the identification of $\mathrm{CFK}^-(\Sigma, \boldsymbol{\alpha}, \boldsymbol{\beta}, \mathbf{w}, \mathbf{z})$ with the mapping
cone of Equation (10). (Note that we broke the symmetry in the construction
by moving q towards α_1 rather than β_1. If we moved q towards β_1 instead, we
would identify $\mathrm{CFK}^-(\Sigma, \boldsymbol{\alpha}, \boldsymbol{\beta}, \mathbf{w}, \mathbf{z})$ with the mapping cone of $U_1 - U_k$.)

For the second assertion of the proposition, view all the U_i as being set to
zero. The above argument shows that

$$C(\Sigma, \boldsymbol{\alpha}, \boldsymbol{\beta}, \mathbf{w}, \mathbf{z}) \cong C(\Sigma', \boldsymbol{\alpha}', \boldsymbol{\beta}', \mathbf{w}', \mathbf{z}') \otimes V;$$

hence a corresponding identification holds on the level of homology. Iterating
this until we remain with two basepoints, we obtain the stated identification.
$\qquad\square$

It is perhaps more traditional to consider the filtration of $\widehat{\mathrm{CF}}(S^3)$ (rather
than CF^-). This filtration is induced from the filtration of $\mathrm{CF}^-(S^3)$ by setting
$U = 0$. According to Proposition 2.3, this filtration is obtained as the induced
filtration of $\mathrm{CFK}^-(\Sigma, \boldsymbol{\alpha}, \boldsymbol{\beta}, \mathbf{w}, \mathbf{z})/U_1$.

2.1. *Modifications for links.* Recall that knot Floer homology has a gen-
eralization to the case of oriented links $\vec{L}$. For an ℓ-component, oriented link

$\vec{L}$ in the three-sphere, this takes the form of a multi-graded theory

$$\widehat{\mathrm{HFL}}(\vec{L}) = \bigoplus_{d \in \mathbb{Z}, h \in \mathbb{H}} \widehat{\mathrm{HFL}}_d(\vec{L}, h),$$

where $\mathbb{H} \cong H_1(S^3 - \vec{L}) \cong \mathbb{Z}^\ell$, with the latter isomorphism induced by an ordering of the link components. Now we sketch the changes to be made to the above discussion for the purposes of understanding link Floer homology for Heegaard diagrams with extra basepoints. Here, "extra" means more than twice ℓ.

Suppose now that $(\Sigma, \boldsymbol{\alpha}, \boldsymbol{\beta}, \mathbf{w}, \mathbf{z})$ is a Heegaard diagram compatible with an oriented link $\vec{L}$ in the sense of Definition 2.1.

We find it convenient to label the basepoints keeping track of which link component they belong to. Specifically, suppose L is a link with ℓ components, and for $i = 1, \ldots, \ell$, we choose k_i basepoints to lie on the ith component. Let S be the index set of pairs (i, j) with $i = 1, \ldots, \ell$ and $j = 1, \ldots, k_i$. Now we have basepoints $\{z_{i,j}\}_{(i,j) \in S}$ and $\{w_{i,j}\}_{(i,j) \in S}$.

We can now form the chain complex $\mathrm{CFL}^-(\Sigma, \boldsymbol{\alpha}, \boldsymbol{\beta}, \mathbf{w}, \mathbf{z})$ defined over $\mathbb{F}[\{U_{i,j}\}_{(i,j) \in S}]$ analogous to the previous version, generated by intersection points of $\mathbb{T}_\alpha \cap \mathbb{T}_\beta$, with differential

$$\partial^- \mathbf{x} = \sum_{\mathbf{y} \in \mathbb{T}_\alpha \cap \mathbb{T}_\beta} \sum_{\{\phi \in \pi_2(\mathbf{x}, \mathbf{y}) \mid \mu(\phi) = 1\}} \# \left(\frac{\mathcal{M}(\phi)}{\mathbb{R}} \right) \cdot \left(\prod_{(i,j) \in S} U_{i,j}^{n_{w_{i,j}}(\phi)} \right) \cdot \mathbf{y}.$$

This complex has a relative Maslov grading, as before. It also has a relative Alexander grading which in this case is an ℓ-tuple of integers

$$A \colon \mathbb{T}_\alpha \cap \mathbb{T}_\beta \longrightarrow \mathbb{Z}^\ell,$$

determined up to an overall additive constant by the formula

$$A(\mathbf{x}) - A(\mathbf{y}) = \left(\sum_{j=1}^{k_1} (n_{z_{1,j}}(\phi) - n_{w_{1,j}}(\phi)), \ldots, \sum_{j=1}^{k_\ell} (n_{z_{\ell,j}}(\phi) - n_{w_{\ell,j}}(\phi)) \right).$$

The indeterminacy in this case is a little more unpleasant to pin down (i.e. one must go beyond the multi-variable Alexander polynomial, which can be identically zero), but it can be done using Proposition 2.5.

The complex $\mathrm{CFL}^-(\Sigma, \boldsymbol{\alpha}, \boldsymbol{\beta}, \mathbf{w}, \mathbf{z})$ inherits an Alexander filtration induced by the Alexander multi-grading of $\mathbb{T}_\alpha \cap \mathbb{T}_\beta$, and the convention that $U_{i,j}$ drops the multi-grading by the ith basis vector. In the case where $k = \ell$, the filtered chain homotopy type of $\mathrm{CFL}^-(\Sigma, \boldsymbol{\alpha}, \boldsymbol{\beta}, \mathbf{w}, \mathbf{z})$ was shown to be a link invariant in [25]; it is the link filtration $\mathrm{CFL}^-(\vec{L})$.

The analogue of $C(\Sigma, \boldsymbol{\alpha}, \boldsymbol{\beta}, \mathbf{w}, \mathbf{z})$ can be defined as well. It is generated by intersection points of $\mathbb{T}_\alpha$ and $\mathbb{T}_\beta$ over $\mathbb{F}$, endowed with the differential

$$\partial \mathbf{x} = \sum_{\mathbf{y} \in \mathbb{T}_\alpha \cap \mathbb{T}_\beta} \sum_{\{\phi \in \pi_2(\mathbf{x}, \mathbf{y}) \mid \substack{\mu(\phi) = 1, \\ n_{w_{i,j}}(\phi) = n_{z_{i,j}}(\phi) = 0 \quad \forall(i,j) \in S}\}} \#\left(\frac{\mathcal{M}(\phi)}{\mathbb{R}}\right) \cdot \mathbf{y}.$$

This differential drops Maslov grading by one and preserves the Alexander multi-grading. Hence the homology groups $H_*(C(\Sigma, \boldsymbol{\alpha}, \mathbf{w}, \mathbf{z}))$ inherit a Maslov grading and an Alexander multi-grading.

PROPOSITION 2.5. *Let* $(\Sigma, \boldsymbol{\alpha}, \boldsymbol{\beta}, \mathbf{w}, \mathbf{z})$ *be a* $2k$-*pointed admissible Heegaard diagram compatible with an oriented link* $\vec{L}$, *with* k_i *pairs of basepoints corresponding to the* i^{th} *component of* $\vec{L}$. *Then, there is a filtered chain homotopy equivalence* $\mathrm{CFL}^-(\Sigma, \boldsymbol{\alpha}, \boldsymbol{\beta}, \mathbf{w}, \mathbf{z})$ *with the usual link filtration* $\mathrm{CFL}^-(\vec{L})$, *viewed as a chain complex over* $\mathbb{F}[\{U_{i,j}\}_{(i,j) \in S}]$. *Moreover, there are* (*relative*) *multi-graded identifications*

$$H(\Sigma, \boldsymbol{\alpha}, \boldsymbol{\beta}, \mathbf{w}, \mathbf{z}) \cong \widehat{HFL}(\vec{L}) \otimes \bigotimes_{i=1}^{\ell} V_i^{\otimes(k_i - 1)},$$

where V_i *is the two-dimensional vector space spanned by one generator in Maslov and Alexander gradings zero, and another in Maslov grading* -1 *and Alexander grading corresponding to minus the* i^{th} *basis vector.*

Proof. This follows as in the proof of Proposition 2.3, with extra care taken to ensure that all Heegaard diagrams remain admissible while performing Heegaard moves, as in [24, Prop. 7.2]. □

3. Proof of Theorem 1.1 and its generalizations

The reader will have noticed by now that the toroidal grid diagrams from the introduction are a special case of the multiply-pointed Heegaard diagrams from Section 2. The Heegaard surface is the torus $\mathcal{T}$, the α-circles are the horizontal circles, and the β-circles are the vertical ones. The basepoints $\{w_i\}_{i=1}^n$ are the white dots, and $\{z_i\}_{i=1}^n$ are the black ones. Since for each i and j, α_i and β_j intersect in the single point (i, j), we see that the generators X are the intersection points of $\mathbb{T}_\alpha$ with $\mathbb{T}_\beta$ in $\mathrm{Sym}^n(\mathcal{T})$. In our coordinate system, these generators can be thought of as graphs of permutations on n letters. To apply the results from Section 2, we must verify the following:

LEMMA 3.1. *The Alexander grading of generators* X, *as specified by the Heegaard diagram given by the grid diagram* (*characterized by Equations* (5) *and* (6)) *coincides with the function* $A \colon X \longrightarrow \mathbb{Z}$ *defined in the introduction* (*Equation* (2)).

Proof. Let A' denote the Alexander grading of generators specified by the Heegaard diagram, and let A denote the function defined in the introduction. Our aim is to show that $A = A'$.

Recall that the Alexander grading A' is determined up to an overall additive constant by the formula

$$A'(\mathbf{x}) - A'(\mathbf{y}) = \left(\sum_{i=1}^{n} n_{z_i}(\phi)\right) - \left(\sum_{i=1}^{n} n_{w_i}(\phi)\right),$$

where $\phi \in \pi_2(\mathbf{x}, \mathbf{y})$ is any homology class connecting $\mathbf{x}$ to $\mathbf{y}$. The right-hand side of this equation can be interpreted as the oriented intersection number of the knot K with the two-chain associated to ϕ, or alternatively as the linking number of K with $\gamma_{\mathbf{x},\mathbf{y}} = \partial \mathcal{D}(\phi)$ (which we think of now as an embedded curve in the three-sphere supported near its Heegaard torus). We can also think of this linking number as the intersection number of a Seifert surface for K with $\gamma_{\mathbf{x},\mathbf{y}}$. Deforming $\gamma_{\mathbf{x},\mathbf{y}}$ (without changing its intersection number with the Seifert surface for K) so that the horizontal segments are far under the Heegaard surface, and the vertical ones are far above it (so that each $x_i \in \mathbf{x}$ is the projection of an arc in $\gamma_{\mathbf{x},\mathbf{y}}$ which points vertically downwards, while each $y_i \in \mathbf{y}$ is the projection of an arc in $\gamma_{\mathbf{x},\mathbf{y}}$ which points vertically upwards), we can arrange that all the intersection points of $\gamma_{\mathbf{x},\mathbf{y}}$ with the Seifert surface occur in the arcs over x_i and y_i. Thus, we have established that for any two generators $\mathbf{x}, \mathbf{y} \in X$,

(11) $$A(\mathbf{x}) - A(\mathbf{y}) = A'(\mathbf{x}) - A'(\mathbf{y}),$$

or equivalently, that there is some κ with the property that for any generator $\mathbf{x} \in X$, $A(\mathbf{x}) = A'(\mathbf{x}) + \kappa$.

The proof that $\kappa = 0$ is elementary, albeit tedious. We sketch it here, leaving the details as an exercise for the interested reader; compare also [16]. One first checks that κ is a knot invariant, by verifying that it is unchanged by vertical and horizontal rotations of the toroidal grid diagram, as well as by the Reidemeister moves from [4] (see also [3]), which relate any two planar grid diagrams of the same knot. Then it suffices to show that the rational function of T determined by the expression

$$Q(K) = \frac{\sum_{\mathbf{x} \in X} T^{A(\mathbf{x})}}{(1 - T^{-1})^{n-1}},$$

which we know is $T^\kappa \cdot \Delta_K(T)$, is actually a symmetric Laurent polynomial in T. This can be done, for example, by verifying that it agrees with the symmetrized Alexander polynomial modulo two, using the skein relation:

$$Q(K_+) - Q(K_-) \equiv (T^{\frac{1}{2}} - T^{-\frac{1}{2}}) \cdot Q(K_0) \pmod 2.$$

The skein relation for Q can be verified readily by realizing the skein moves in grid position. Finally, a straightforward calculation in a 2×2 diagram shows

that $Q(K) = 1$ when K is the unknot. It follows that $Q(K)$ is the symmetrized Alexander polynomial modulo two, and in particular that Q is symmetric. $\square$

LEMMA 3.2. *The Maslov grading of generators X, as specified by the Heegaard diagram $(\mathcal{T}, \{\alpha_1, \ldots, \alpha_n\}, \{\beta_1, \ldots, \beta_n\}, \{w_1, \ldots, w_n\}, \{z_1, \ldots, z_n\})$ and characterized by Equations (7) and (8), coincides with the function $M \colon X \longrightarrow \mathbb{Z}$ defined in the introduction (characterized by Equation (3) and the normalization that $M(\mathbf{x}_0) = 1 - n$).*

Proof. For $\phi \in \pi_2(\mathbf{x}, \mathbf{y})$, we claim that its Maslov index $\mu(\phi)$ is given by the formula

$$(12) \qquad \mu(\phi) = P_{\mathbf{x}}(\mathcal{D}(\phi)) + P_{\mathbf{y}}(\mathcal{D}(\phi)).$$

This is a particular case of Lipshitz's formula for the Maslov index in an arbitrary Heegaard diagram [14]. However, for domains on a grid diagram, we can also give an elementary proof as follows.

Let $\mu'(\phi)$ denote the quantity on the right-hand side of Equation (12). First, note that $\mu'(\phi) = 1$ when the domain $\mathcal{D}(\phi)$ associated to a homology class $\phi \in \pi_2(\mathbf{x}, \mathbf{y})$ is a rectangle r in the torus which contains none of the components of $\mathbf{x}$ in its interior. In this case we also have $\mu(\phi) = 1$, because the moduli space of complex structures on a disk with four marked points on the boundary is one-dimensional.

Next, consider the natural map given by juxtaposition of flow lines:

$$* : \pi_2(\mathbf{x}, \mathbf{y}) \times \pi_2(\mathbf{y}, \mathbf{z}) \to \pi_2(\mathbf{x}, \mathbf{z}).$$

The Maslov index is additive under this operation, i.e. $\mu(\phi_1 * \phi_2) = \mu(\phi_1) + \mu(\phi_2)$. We claim that the same is true for μ'. Indeed, the relation

$$P_{\mathbf{x}}(\mathcal{D}(\phi_1)) + P_{\mathbf{y}}(\mathcal{D}(\phi_1)) + P_{\mathbf{y}}(\mathcal{D}(\phi_2)) + P_{\mathbf{z}}(\mathcal{D}(\phi_2))$$
$$= P_{\mathbf{x}}(\mathcal{D}(\phi_1 * \phi_2)) + P_{\mathbf{z}}(\mathcal{D}(\phi_1 * \phi_2))$$

is equivalent to

$$(13) \qquad P_{\mathbf{x}}(\mathcal{D}(\phi_2)) - P_{\mathbf{y}}(\mathcal{D}(\phi_2)) = P_{\mathbf{y}}(\mathcal{D}(\phi_1)) - P_{\mathbf{z}}(\mathcal{D}(\phi_1)).$$

Let $\gamma_{\mathbf{x},\mathbf{y}}^{NE}, \gamma_{\mathbf{x},\mathbf{y}}^{NW}, \gamma_{\mathbf{x},\mathbf{y}}^{SW}, \gamma_{\mathbf{x},\mathbf{y}}^{SE}$ denote small translates of the curve $\gamma_{\mathbf{x},\mathbf{y}} = \partial \mathcal{D}(\phi_1)$ on the torus, in the four diagonal directions. As in the proof of Lemma 3.1, we deform these curves by pushing their horizontal arcs under the Heegaard surface and their vertical arcs above the Heegaard surface; thus we can think of them as embedded curves in the three-sphere. The left-hand side of Equation (13) is then the average of the intersection numbers of the surface $\mathcal{D}(\phi_2)$ with each of $\gamma_{\mathbf{x},\mathbf{y}}^{NE}, \gamma_{\mathbf{x},\mathbf{y}}^{NW}, \gamma_{\mathbf{x},\mathbf{y}}^{SW}, \gamma_{\mathbf{x},\mathbf{y}}^{SE}$. Alternatively, it can be viewed as the average linking number of $\gamma_{\mathbf{y},\mathbf{z}} = \partial \mathcal{D}(\phi_2)$ with these four curves. The
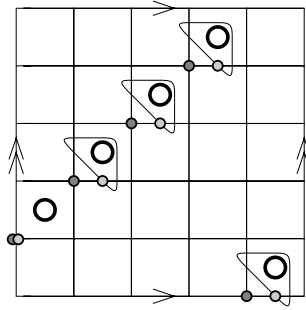
Figure 8: *Fixing the Maslov grading.* Handleslide the vertical circles from left to right, to obtain the smaller null-homotopic circles β_i' encircling the various w_i. There is a collection of triangles connecting the generator $\mathbf{x}_0$, indicated here with the darkly shaded circles, with the bottom-most generator of $\mathbb{T}_\alpha \cap \mathbb{T}_\beta'$, indicated here with the lightly shaded circles.

right-hand side of (13) has a similar interpretation. Since the linking number is symmetric, the two sides are equal. Therefore, μ' is additive under juxtaposition of flow lines.

Now, given an arbitrary pair $\mathbf{x}, \mathbf{y} \in X$, it is easy to construct a sequence of generators $\mathbf{x}_1, \ldots, \mathbf{x}_m \subset X$ with $\mathbf{x} = \mathbf{x}_1$, $\mathbf{y} = \mathbf{x}_m$, and $\phi_i \in \pi_2(\mathbf{x}_i, \mathbf{x}_{i+1})$ with the property that $\mathcal{D}(\phi_i)$ is a rectangle with no components of $\mathbf{x}_i$ in its interior. It follows that if we let $\psi = \phi_1 * \cdots * \phi_m$, then $M(\psi) = M'(\psi)$. The alpha curves cut the torus into n annuli $\{A_i\}_{i=1}^n$, and similarly the beta curves cut it into annuli $\{B_i\}_{i=1}^n$. The homology classes ψ and ϕ differ by adding or subtracting some number of copies of annuli A_i or B_j (thought of as elements of $\pi_2(\mathbf{x}, \mathbf{x})$), for which $\mu(A_i) = \mu'(A_i) = 2$ (because A_i can be decomposed as a juxtapositon of two rectangles). It follows that $\mu(\phi) = \mu(\phi')$.

We have verified Equation (12). It follows now that the relative Maslov grading from Equation (7) specializes to Equation (3).

We can lift from the relative to the absolute Maslov grading by performing handleslides on the β-circles in our diagram which now are allowed to cross the z_i, to reduce to a diagram which has 2^{n-1} intersection points in $\mathbb{T}_\alpha \cap \mathbb{T}_\beta'$, and for which all the differentials in the chain complex vanish; indeed, it is identified with the homology of an $n-1$-dimensional torus. The handleslides are performed by successively handlesliding β_i over β_{i+1} for $i = 1, \ldots, n-1$, as pictured in Figure 8. Now it is easy see that the generator $\mathbf{x}_0$ from the introduction can be connected to the bottom-most generator of the new chain complex by a collection of (Maslov index zero) triangles. According to (8), the grading of $\mathbf{x}_0$ should be $1 - n$. □

We can now turn to the following:

Proof of Theorem 1.1.   The fact that the Alexander and Maslov gradings are identified has been verified in Lemmas 3.2 and 3.1 above. It remains to identify the differentials.

The circles $\alpha_1, \ldots, \alpha_n$ and $\beta_1, \ldots, \beta_n$ cut up $\mathcal{T}$ into n^2 squares $D_{i,j}$ with $1 \leq i, j \leq n$. According to [24, Prop. 2.15], homology classes of Whitney disks $\phi \in \pi_2(\mathbf{x}, \mathbf{y})$ are determined by their underlying two-chain

$$\mathcal{D}(\phi) = \sum_{i,j} a_{ij} D_{i,j},$$

where here $a_{i,j} = n_{p_{i,j}}(\phi)$ for some point $p_{i,j} \in D_{i,j}$. Indeed, if $\mathbf{x}$ and $\mathbf{y}$ correspond to permutations σ and τ, then these induced two-chains are the ones that satisfy the property for all $i = 1, \ldots, n$ that

$$\partial(\partial \mathcal{D}(\phi) \cap \alpha_i) = (i, \tau(i)) - (i, \sigma(i)).$$

To understand the differential, we must count holomorphic disks in $\mathcal{M}(\phi)$ with $\mu(\phi) = 1$. First, we classify all nonnegative homology classes ϕ with Maslov index one.

Let $D = \mathcal{D}(\phi)$. First observe that if ∂D is 0 on $(n-1)$ α circles, then it is in fact 0 on all the α circles, and D is generated by the annular regions cut out by the β circles. Now, if such a thing happens then $\mathbf{x} = \mathbf{y}$, and its Maslov index is even.

Thus we can assume that ∂D is nonzero on at least two α circles (say α_{j_1} and α_{j_2}) and similarly nonzero on at least two β circles (β_{i_1} and β_{i_2}). It follows that there are permutations σ and τ such that

$$P_{\mathbf{x}}(D) \geq p_{(i_1, \sigma(i_1))}(D) + p_{i_2, \sigma(i_2)}(D) \geq 1/2,$$
$$P_{\mathbf{y}}(D) \geq p_{(i_1, \tau(i_1))}(D) + p_{i_2, \tau(i_2)}(D) \geq 1/2.$$

Since $\mu(\phi) = P_{\mathbf{x}}(D) + P_{\mathbf{y}}(D) = 1$, equality must hold throughout. It follows that ∂D is nonzero precisely on $\alpha_{j_1}, \alpha_{j_2}, \beta_{i_1}$ and β_{i_2}, and D is one of the two rectangles with four vertices (i_1, j_1), (i_1, j_2), (i_2, j_1), and (i_2, j_2). Without loss of generality, assume $\sigma(i_1) = j_1$ and $\sigma(i_2) = j_2$. Then $\tau(i_1) = j_2$ and $\tau(i_2) = j_1$, and it agrees with σ on the rest of the values. Also for the Maslov index requirement, $(i, \sigma(i)) = (i, \tau(i))$ does not lie in the interior of D for any other i.

Thus, we have established that the only $\phi \in \pi_2(\mathbf{x}, \mathbf{y})$ with nonnegative local multiplicities and Maslov index equal to one are those whose underlying domain r is a rectangle of the form $r \in R_{\mathbf{x},\mathbf{y}}$ with $P_{\mathbf{x}}(r) + P_{\mathbf{y}}(r) = 1$. Moreover, we claim that in this case, the number of pseudo-holomorphic representatives of r is odd. In fact, this can be seen by elementary complex analysis, using a (classical) complex structure on the symmetric product of $\mathcal{T}$, where one shows that in fact the moduli space consists of a single representative. Indeed, for this choice, the moduli space $\mathcal{M}(r)/\mathbb{R}$ can be seen to correspond to involutions

of r (with the complex structure it inherits from $\mathcal{T}$) which switch opposite sides of the rectangle. It is a simple exercise in conformal geometry that for any rectangle, there is a unique such involution.

We have completed the verification that the complex $C(\Gamma)$ from the introduction coincides with the Heegaard Floer complex $C(\mathcal{T}, \boldsymbol{\alpha}, \boldsymbol{\beta}, \mathbf{w}, \mathbf{z})$ in the notation of Section 2. Theorem 1.1 now follows directly from Proposition 2.3 (Equation (9)). □

3.1. *Other variants.* There are other variants of Theorem 1.1, which should be clear from the constructions thus far. We state several of them for completeness.

Label the white dots $\{w_1, \ldots, w_n\}$, and let $n_{w_i}(r)$ denote the local multiplicity of r at w_i. Consider the chain complex $C^-(\Gamma)$ over the algebra $\mathbb{F}[U_1, \ldots, U_n]$ also generated by X, endowed with the differential

$$\partial^- \mathbf{x} = \sum_{\mathbf{y} \in X} \sum_{r \in R_{\mathbf{x},\mathbf{y}}} \left\{ \begin{array}{ll} 1 & \text{if } P_{\mathbf{x}}(r) + P_{\mathbf{y}}(r) = 1 \\ 0 & \text{otherwise} \end{array} \right\} U_1^{n_{w_1}(r)} \cdot \ldots \cdot U_n^{n_{w_n}(r)} \cdot \mathbf{y},$$

thought of as a filtered chain complex where the filtration level of each generator $\mathbf{x} \in X$ is its Alexander grading, and multiplication by the variable U_i drops filtration level by one.

THEOREM 3.3. *Fix a grid presentation Γ of a knot K, with grid number n. The filtered chain homotopy type of K coincides with the filtered chain homotopy type of the knot filtration $\mathrm{CF}^-(S^3, K)$.*

Proof. The proof of Theorem 1.1 identifies the filtered chain complex $C^-(\Gamma)$ with the complex denoted $\mathrm{CFK}^-(\mathcal{T}, \boldsymbol{\alpha}, \boldsymbol{\beta}, \mathbf{w}, \mathbf{z})$ in Section 2 which, by Proposition 2.3, is identified with $\mathrm{CFK}^-(K)$. □

The other filtrations $\mathrm{CFK}^\infty(S^3, K)$ and $\mathrm{CFK}^+(S^3, K)$ from [23] can be extracted from this information.

We call attention to another other construction, which gives a concordance invariant $\tau(K)$ for knots [21], [27]. This is a homomorphism from the smooth concordance group of knots to the integers, which can be used to bound the four-ball genus of knots, giving an alternate proof of the theorem of Kronheimer and Mrowka [13] confirming Milnor's conjecture for the unknotting numbers of torus knots. This feature underscores its similarity with Rasmussen's concordance invariant $s(K)$ [28] from Khovanov homology [12]. However, these two invariants are known to be linearly independent [11].

Recall that the filtration $\mathrm{CFK}^-(K)$ of $\mathrm{CF}^-(S^3)$ also induces a filtration $\{\widehat{\mathcal{F}}_m(S^3)\}_{m \in \mathbb{Z}}$ of $\widehat{\mathrm{CF}}(S^3) = \mathrm{CF}^-(S^3)/U \cdot \mathrm{CF}^-(S^3)$. The concordance invariant $\tau(K)$ is by definition the minimal $m \in \mathbb{Z}$ with the property that the map

$$H_*(\widehat{\mathcal{F}}_m(S^3)) \longrightarrow \widehat{\mathrm{HF}}(S^3) \cong \mathbb{F}$$

is nontrivial.

We have a corresponding chain complex $\widehat{C}(\Gamma) = \mathrm{CF}^-(\Gamma)/U_1 \cdot \mathrm{CF}^-(\Gamma)$, i.e. whose differential is given by

$$\widehat{\partial}\mathbf{x} = \sum_{\mathbf{y} \in X} \sum_{r \in R_{\mathbf{x},\mathbf{y}}} \left\{ \begin{array}{ll} 1 & \text{if } P_{\mathbf{x}}(r) + P_{\mathbf{y}}(r) = 1 \text{ and } n_{w_1}(r) = 0 \\ 0 & \text{otherwise} \end{array} \right\} U_2^{n_{w_2}(r)} \cdot \ldots \cdot U_n^{n_{w_n}(r)} \cdot \mathbf{y}.$$

This is equipped with subcomplexes $\widehat{F}(K, m) \subset \widehat{C}(\Gamma)$, generated by elements $U_2^{a_2} \cdot \ldots \cdot U_n^{a_n} \cdot \mathbf{x}$ with integral $a_i \geq 0$, and

$$A(\mathbf{x}) - a_2 - \cdots - a_n \leq m.$$

COROLLARY 3.4. *The concordance invariant $\tau(K)$ is the minimal m for which the map induced on homology*

$$i_* \colon H_*(\widehat{\mathcal{F}}(K, m)) \longrightarrow H_*(\widehat{C}(\Gamma))$$

is nontrivial.

Proof. Theorem 3.3 actually gives an identification of the filtered chain homotopy type of $\widehat{\mathrm{CFK}}(K)$ with $\widehat{C}(\Gamma)$. The result then follows from the definition of $\tau(K)$. $\square$

Consider now the case of link Floer homology. In order to use the Heegaard diagram associated to a grid diagram to calculate link Floer homology, we must verify that it is admissible.

LEMMA 3.5. *The diagram*

$$(\mathcal{T}, \{\alpha_1, \ldots, \alpha_n\}, \{\beta_1, \ldots, \beta_n\}, \{w_1, \ldots, w_n\}, \{z_1, \ldots, z_n\})$$

is admissible.

Proof. The formal differences $A_i - B_i$ span the space of periodic domains. Drawing $\mathcal{T}$ as a square, with equally spaced vertical and horizontal circles, it follows that the total signed area of any periodic domain is zero. Clearly, a nonzero region with this property must have both positive and negative local multiplicities. $\square$

For the case of links, we number our dots $\{w_{i,j}\}_{(i,j) \in S}$ and $\{z_{i,j}\}_{(i,j) \in S}$ where S is the index set consisting of (i, j) with $i = 1, \ldots, \ell$ and $j = 1, \ldots, n_i$, and the dots $w_{i,j}$ and $z_{i,j}$ lie on the ith component of $\vec{L}$.

In this case, the Alexander grading is an ℓ-tuple of integers. It is uniquely characterized by the property that for $\mathbf{x}, \mathbf{y} \in X$, the ith component of the Alexander grading is the winding number of $\gamma_{\mathbf{x},\mathbf{y}}$ about the sum of the black dots in $\{z_{i,j}\}_{(i,j) \in S}$ minus its winding number around $\{w_{i,j}\}_{(i,j) \in S}$. Again, this can be more succinctly recorded by placing (minus one time) a vector of winding numbers at each vertex, and defining $A(\mathbf{x})$ as the sum of these local
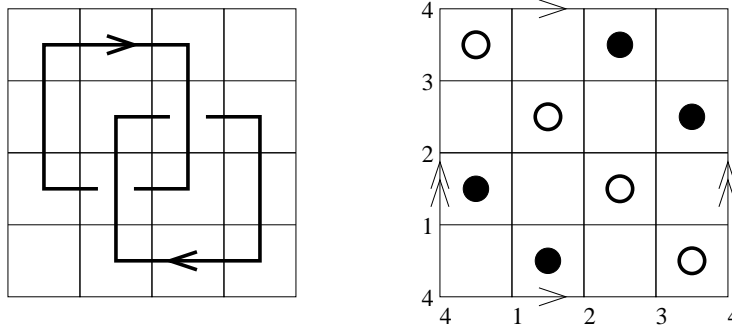
Figure 9: *Grid presentation of the Hopf link.*

contributions at each intersection point in **x**. This can then be renormalized
to be symmetric.

Once again, we have the chain complex $C(\Gamma)$ as defined in the introduc-
tion, which now inherits an ℓ-tuple of Alexander gradings and a single Maslov
grading. There is also a refinement, $C^-(\Gamma)$, which is freely generated by X
over $\mathbb{F}[\{U_{i,j}\}_{(i,j)\in S}]$, endowed with the differential

$$\partial^- \mathbf{x} = \sum_{\mathbf{y}\in X} \sum_{r\in R_{\mathbf{x},\mathbf{y}}} \left\{ \begin{array}{ll} 1 & \text{if } P_{\mathbf{x}}(r) + P_{\mathbf{y}}(r) = 1 \\ 0 & \text{otherwise} \end{array} \right\} \cdot \left(\prod_{(i,j)\in S} U_{i,j}^{n_{w_{i,j}}(r)} \right).$$

THEOREM 3.6. *There are multi-graded identifications*

$$H_*(C(\Gamma), \partial) \cong \widehat{HFL}(\vec{L}) \otimes \bigotimes_{i=1}^{\ell} V_i^{\otimes(n_i-1)},$$

*where V_i is the two-dimensional vector space spanned by two generators, one
in zero Maslov and Alexander multigradings, and the other in Maslov grading
negative one and Alexander multi-grading corresponding to minus the ith basis
vector. More generally, the multi-filtered chain homotopy type of $\text{CFL}^-(S^3, \vec{L})$
is identified with the multi-filtered chain homotopy type of $C^-(\Gamma)$.*

Proof. This follows from the proof of Theorem 1.1, combined with Propo-
sition 2.5.   □

4. Examples

We give a few elementary illustrations of our results.

4.1. *Hopf link.* Consider the grid presentation Γ for the Hopf link with
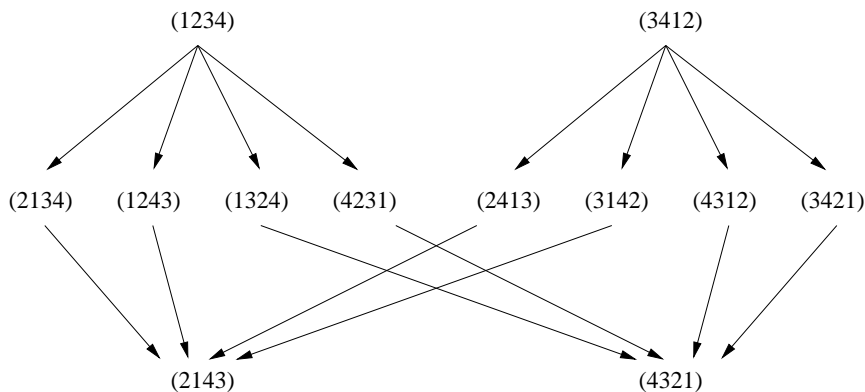grid number $n = 4$, shown in Figure 9.

Figure 10: *Part of the chain complex for the Hopf link.* This complex appears in Alexander bigrading $(-\frac{1}{2}, -\frac{1}{2})$. Its homology has rank four.

The generators of the chain complex $C(\Gamma)$ are in one-to-one correspondence with permutations σ of the set $\{1, 2, 3, 4\}$. For conciseness, we write the generator consisting of the intersections of the ith horizontal circle with the $\sigma(i)^{\text{th}}$ vertical circle as $\big(\sigma(1)\sigma(2)\sigma(3)\sigma(4)\big)$.

There are eight empty squares in the grid. Each of them produces differentials between generators that differ by a transposition, according to the recipe:

$$
\begin{array}{cccc}
(1\ 2\ *\ *) & (*\ 2\ 3\ *) & (*\ *\ 3\ 4) & (1\ *\ *\ 4) \\
\downarrow & \downarrow & \downarrow & \downarrow \\
(2\ 1\ *\ *) & (*\ 3\ 2\ *) & (*\ *\ 4\ 3) & (4\ *\ *\ 1)
\end{array}
$$

$$
\begin{array}{cccc}
(3\ 4\ *\ *) & (*\ 4\ 1\ *) & (*\ *\ 1\ 2) & (3\ *\ *\ 2) \\
\downarrow & \downarrow & \downarrow & \downarrow \\
(4\ 3\ *\ *) & (*\ 1\ 4\ *) & (*\ *\ 2\ 1) & (2\ *\ *\ 3).
\end{array}
$$

The result is that there are sixteen differentials in $(C(\Gamma), \partial)$. They connect twelve of the 24 generators, as shown schematically in Figure 10. Each of the other twelve generators is not connected by differentials to any other generators. Therefore, the homology of our complex has total rank $4 + 12 = 16$.

The Alexander bigrading of the generators is computed using the adaptation for links of Equation (2). For example,

$$
A(3214) = \Big(\frac{1}{2}, \frac{1}{2}\Big), \quad A(2143) = \Big(-\frac{1}{2}, -\frac{1}{2}\Big).
$$

To compute the Maslov gradings, we start with the canonical generator (2143), which has $M = -3$. Then, we relate each of the other generators to

the canonical one by a sequence of transpositions. Whenever two generators $\mathbf{x}$ and $\mathbf{y}$ differ by a transposition, if a two-chain D has boundary $\gamma_{\mathbf{x},\mathbf{y}}$, then D consists of two points and a rectangle, and it is straightforward to apply Equation (3). For example,

$$M(2134) = M(2143) + 1 = -2, \quad M(2314) = M(2134) + 1 = -1, \text{ etc.}$$

The result is that

$$H_*(C(\Gamma), \partial) = \left(V_1^{\otimes 2} \otimes V_2^{\otimes 2} \right) \left[\frac{1}{2}, \frac{1}{2} \right].$$

Here, the notation $[i, j]$ denotes an upward shift in Alexander bigrading, i.e. if V is a bigraded vector space, then $(V[i, j])_{x,y} = V_{x-i,y-j}$. The link Floer homology of $\vec{H}$ is $(V_1 \otimes V_2)[\frac{1}{2}, \frac{1}{2}]$, cf. [25]. This confirms that

$$H_*(C(\Gamma), \partial) = \widehat{\mathrm{HFL}}(\vec{H}) \otimes V_1 \otimes V_2.$$

4.2. *The trefoil.* Consider the grid presentation of the trefoil knot shown in Section 1. There are 120 generators of the chain complex. A quick glance at Figure 1 reveals 15 rectangles containing no black or white dot: fifteen 1×1, five 2×1, and five 1×2. Each rectangle gives rise to $3! = 6$ different differentials. With a little computer assistance or a great deal of patience, one finds that the homology of this complex has rank 48. Indeed, with the conventions used in Subsection 4.1, one finds that the generators correspond to permutations (listed in increasing Alexander grading):

(23451)	(13452)	(23415)	(23541)	(24351)	(32451)	(13542)	(14352)
(24153)	(24315)	(25413)	(32415)	(32541)	(35421)	(42351)	(43152)
(43521)	(15342)	(15423)	(25143)	(31542)	(32514)	(35241)	(41352)
(42153)	(42315)	(43125)	(45321)	(52341)	(52413)	(54312)	(15243)
(15324)	(31524)	(41325)	(42135)	(51342)	(51423)	(52143)	(52314)
(54132)	(54213)	(15234)	(41235)	(51243)	(51324)	(52134)	(51234).

These generators have Alexander gradings between -5 and 1. There are $1, 5, 11,$
$14, 11, 5, 1$ generators in gradings $-5, -4, -3, -2, -1, 0, 1$, respectively. The knot Floer homology group for the left-handed trefoil T is nontrivial in only three Alexander-Maslov bigradings: $(-1, 0)$, $(0, 1)$, and $(1, 2)$. It has rank one in these three bigradings. Considering Maslov gradings as well, one verifies that

$$H_*(C(\Gamma)) \cong \widehat{\mathrm{HFK}}(T) \otimes V^{\otimes 4}.$$

COLUMBIA UNIVERSITY, NEW YORK, NY
E-mail addresses: cm@math.columbia.edu
                    petero@math.columbia.edu

PRINCETON UNIVERISTY, PRINCETON, NJ
E-mail address: sucharit@math.princeton.edu

References

[1]   H. Brunn, Über verknotete Kurven, *Verhandlungen des Internationalen Math. Kongresses* (Zurich 1897), pp. 256–259, 1898.

[2]   Y. Chekanov, Differential algebra of Legendrian links, *Invent. Math.* **150** (2002), 441–483.

[3]   P. R. Cromwell, Embedding knots and links in an open book. I. Basic properties, *Topology Appl.* **64** (1995), 37–58.

[4]   I. Dynnikov, Arc-presentations of links: monotonic simplification, *Fund. Math.* **190** (2006), 29–76.

[5]   Y. Eliashberg, Invariants in contact topology, In *Proceedings of the International Congress of Mathematicians*, Vol. II (Berlin, 1998), Extra Vol. II, pp. 327–338 (electronic), 1998.

[6]   A. Floer, Morse theory for Lagrangian intersections, *J. Differential Geometry* **28** (1988), 513–547.

[7]   ———, The unregularized gradient flow of the symplectic action, *Comm. Pure Appl. Math.* **41** (1988), 775–813.

[8]   A. Floer, H. Hofer, and D. Salamon, Transversality in elliptic Morse theory for the symplectic action, *Duke Math. J.* **80** (1995), 251–29.

[9]   K. Fukaya, Y-G. Oh, K. Ono, and H. Ohta, *Lagrangian intersection Floer theory—anomaly and obstruction*, Kyoto University, 2000.

[10] P. Ghiggini, Knot Floer homology detects genus-one fibred links, *Amer. J. Math.* **130** (2008), 1151–1169.

[11] M. Hedden and P. Ording, The Ozsváth-Szabó and Rasmussen concordance invariants are not equal, *Amer. J. Math.* **130** (2008), 441–453.

[12] M. Khovanov, A categorification of the Jones polynomial, *Duke Math. J.* **101** (2000), 359–426.

[13] P. B. Kronheimer and T. S. Mrowka, Gauge theory for embedded surfaces. I, *Topology* **32** (1993), 773–826.

[14] R. Lipshitz, A cylindrical reformulation of Heegaard Floer homology, *Geom. Topol.* **10** (2006), 955–1097 (electronic).

[15] H. C. Lyon, Torus knots in the complements of links and surfaces, *Michigan Math. J.*, **27** (1980), 39–46.

[16] C. Manolescu, P. S. Ozsváth, Z. Szabó, and D. P. Thurston, On combinatorial link Floer homology, *Geom. Topol.* **11** (2007), 2339–2412.

[17] H. Matsuda, Links in an open book decomposition and in the standard contact structure, *Proc. Amer. Math. Soc.*, 2006.

[18] L. Ng, Computable Legendrian invariants, *Topology* **42** (2003), 55–82.

[19] Y. Ni, Knot Floer homology detects fibred knots, *Invent. Math.* **170** (2007), 577–608.

[20] Y-G. Oh, On the structure of pseudo-holomorphic discs with totally real boundary conditions, *J. Geom. Anal.* **7** (1997), 305–327.

[21] P. S. Ozsváth and Z. Szabó, Knot Floer homology and the four-ball genus, *Geom. Topol.* **7** (2003), 615–639.

[22] ———, Holomorphic disks and genus bounds, *Geom. Topol.* **8** (2004), 311–334.

[23] ———, Holomorphic disks and knot invariants, *Adv. Math.* **186** (2004), 58–116.

[24] P. S. Ozsváth and Z. Szabó, Holomorphic disks and topological invariants for closed three-manifolds, *Ann. of Math.* **159** (2004), 1027–1158.

[25] ———, Holomorphic disks, link invariants, and the multi-variable Alexander polynomial, *Alg. Geom. Top.* **8** (2008), 615–692.

[26] ———, Knot Floer homology and rational surgeries, math.GT/0504404, 2005.

[27] J. A. Rasmussen, *Floer homology and knot complements*, Ph.D. thesis, Harvard University, 2003.

[28] ———, Khovanov homology and the slice genus, math.GT/0402131, 2004.

[29] S. Sarkar and J. Wang, A combinatorial description of some Heegaard Floer homologies, *Ann. of Math.*, to appear.